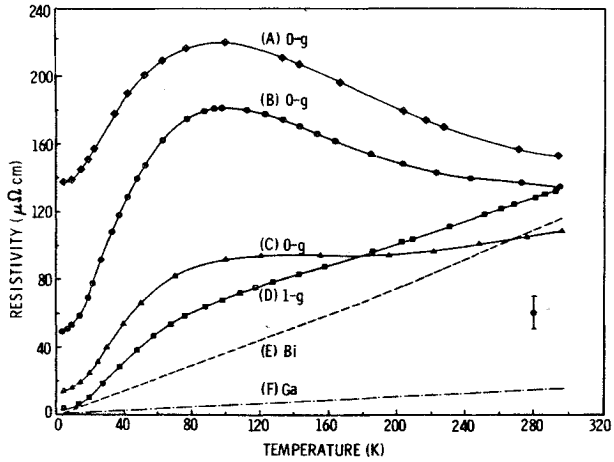

Fig. 2 The temperature dependence of the electrical resistivity of the zero-g and one-g solidified samples. Curves E and F are for the pure elements Bi and Ga, respectively.

loaded-copper wires contacted to the sample bases by silver conductive paint. The voltage drop was measured on two separate potential leads and could be recorded as a function of temperature. The sample temperature was measured with a calibrated platinum resistance thermometer to 20 K and below this temperature with a calibrated Ge resistance thermometer.

The results of the resistivity measurements $\rho(T)$ are given in Fig. 2. Each letter refers to the same samples as identified in Fig. 1. The results clearly show that the resistivity of the zero-g samples A, B, and C is quite different from the ground control sample D. For comparison, the resistivities for pure Bi (curve E) and pure Ga (curve F) have also been included. The room temperature (295 K) value for all samples is approximately the same as for the pure Bi. An absolute determination of ρ for all samples is limited by the small sample geometry to within 8%, indicated by the room temperature error bar. However, the relative values of ρ for a given curve are accurate to within 1%. What is of interest here is that the changes in resistivity as a function of temperature for the three samples are quite different.

The slope $(d\rho/dT)$ for the curves D, E, and F are all positive which is typical of normal conductors. Note that the coarse dispersion of the ground control sample D has given a material with the same electrical characteristics as for pure Bi. However, when the dimensions or diameter of the dispersed Ga particles in sample C become small (3–10 μm), the electrical characteristics of the Bi matrix have changed (i.e., $d\rho/dT \approx 0$). For even smaller dispersions ($d \gtrsim 1$ μm) as seen in the zero-g samples A and B, the conductivity of the matrix has completely changed such that $d\rho/dT < 0$, and a broad maximum occurs at 100 K. The high temperature resistivity of samples A and B behaves similar to an intrinsic semiconductor. As can be seen in the photomicrographs, there is a correlation between the size of the Ga particles and the resistivity curves of Fig. 2.

In the low temperature region between 25 and 4.2 K, all samples show typical metallic behavior. In accordance with Matthiessen's rule,[8] the temperature-dependent resistivity may be expressed as the sum of a temperature-independent term, ρ_o, and a temperature-dependent (intrinsic) term $\rho_i(T)$. Thus, the resistivity may be expressed as

$$\rho(T) = \rho_o + \rho_i(T) \tag{1}$$

where the intrinsic term is usually found to be

$$\rho_i(T) = CT^n \tag{2}$$

The value of ρ_o can be associated with electron scattering from impurities, defects, or interfaces and is indeed very high for sample A, having the finest dispersion. From Fig. 2, it can be seen that ρ_o increases as the particle size becomes smaller, indicating that ρ_o is correlated with the interface area of the Ga particles. The temperature-dependent term for all samples could be expressed by Eq. (2) with n varying between 2 for pure Bi and 4 for pure Ga. What is indeed surprising about this material is that for the same chemical composition, both ρ_o and ρ_i depend upon the degree or fineness of the dispersion.

Similar resistivity peaks have been reported by Thompson[9] for Bi samples doped with Pb, Sn, and Ge. It should be noted, however, that our results are not expected to be influenced by impurity effects, since very pure materials were used and since the resistivity peak does not occur for the ground control sample.

In summary, our results show that the electrical properties of the Bi matrix are drastically changed by zero-g processing, and that the electrical properties can be correlated with the degree of dispersion obtained as shown in the photomicrographs. The finer the dispersion, the more pronounced is the change in the properties of the composite. Even with the short duration of zero-g obtained in a drop tower,‡ useful solidification experiments can be performed with immiscible alloys. Additional investigations with Ga-Bi for longer solidification times are presently being carried out to obtain even finer dispersions.

References

[1] Reger, J. L., "Study on Processing Immiscible Materials in Zero-Gravity," Interim Report on NASA Contract NAS8-28267, May 1973, TRW Systems Group, Redondo Beach, Calif.

[2] Lacy, L. L. and Otto, G. H., "The Behavior of Immiscible Liquids in Space," AIAA/ASME Paper 74-668, Boston, Mass., 1974.

[3] Yates, I. C., "Apollo 14 Composite Casting Demonstration," TM X-64641, March 1972, NASA.

[4] Reger, J. L., "Immiscible Alloy Compositions," *Proceedings of the Third Space Processing Symposium—Skylab Results,* Marshall Space Flight Center, Huntsville, Ala., Vol. 1, 1974, pp. 133–158.

[5] Reger, J. L., "Experiment Development of Processes to Produce Homogenized Alloys of Immiscible Metals," Final Report on NASA Contract NAS8-27085, Jan. 1973, TRW Systems Group, Redondo Beach, Calif.

[6] Otto, G. H. and Lacy, L. L., "Electrical Properties of Low-G Processed Immiscible Alloys," *Proceedings of the Third Space Processing Symposium—Skylab Results,* Marshall Space Flight Center, Huntsville, Ala., Vol. 2, 1974, pp. 1031–1044.

[7] Yost, V. H., "Drop Towers and Research Rockets for Space Processing," AIAA/ASME Paper 74-648, Boston, Mass., 1974.

[8] Wilson, A. H., *The Theory of Metals,* 2nd ed., Cambridge University Press, New York, 1965.

[9] Thompson, N., "The Electrical Resistance of Bismuth Alloys," *Proceedings of the Royal Society, London,* Ser. A, Vol. 155, 1963, pp. 111–123.

‡ The actual acceleration levels in the MSFC drop tower are approximately 10^{-3} g and are here referred to as "zero-g" or "low-g."

Solution of an Eigenvalue Problem in Solid Mechanics Employing Parameter Differentiation

T. Y. NA* AND G. M. KURAJIAN†
The University of Michigan, Dearborn, Mich.

Introduction

IN a previous paper by the authors,[1] an initial value method for solving the eigenvalue problem resulting from the analysis of the finite deflections of a nonlinearly elastic bar,[2] clamped at one end and axially loaded at the other (Fig. 1) was treated.

Received March 22, 1974; revision received July 26, 1974.
Index category: Structural Static Analysis.
* Professor of Mechanical Engineering. Associate Member AIAA.
† Professor of Mechanical Engineering.

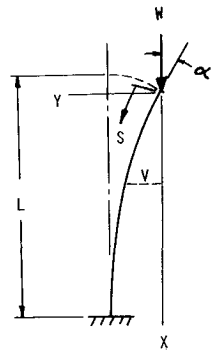

Fig. 1 The bar.

In this Note, the method of parameter differentiation[3-7] is employed to solve the same problem. The same problem was selected so that a comparison could be more easily accomplished. This *noniterative* method is applied to seek a family of solutions of the equations involving an assignment of a realistic *range* of values of the parameter. Beginning with a given set of solutions for a particular value of the parameter, solutions for a range of values of that parameter are obtained by integrating the rate of change of the solution with respect to this parameter.

Thus, it is the objective of this Note to not only present another noniterative method for solving such problems, but also to demonstrate its accuracy, versatility, and simplicity as was the case of the method of transformation groups.[1] Even though the method of parameter differentiation has been applied to problems in other areas,[3-7] application of this method to the solution of eigenvalue problems in solid mechanics has not been treated in the literature.

Problem Statement and Parameter Differentiation

The physical problem under consideration is a nonlinearly elastic bar clamped at one end and axially loaded at the free end, as shown in Fig. 1. The nonlinearly elastic material is assumed to be characterized by a moment curvature law similar to that exhibited by a class of elastoplastic materials which can be written as

$$M = (D_0 - D_1)\phi_0 \tanh\left(\frac{\phi}{\phi_0}\right) + D_1\phi$$

where D_0 and D_1 are the characteristic flexural rigidities and ϕ_0 is a material constant. The function ϕ is a characteristic change-in-curvature.

Let α, ϕ, and θ denote the slope of the deflection curve at the free end, the change-in-curvature and the slope of the bar at any location, respectively. The eigenvalue problem can be stated as follows: Given the deflection angle, α, at the free end, determine the load parameter, (λ), required to maintain a given deflection curve.

The following system of differential equations results from the analysis of the finite deflections of the nonlinearly elastic bar shown in Fig. 1[2]:

$$du/dz = \sin\theta \qquad d\theta/dz = \psi \quad , \quad d\lambda/dz = 0 \tag{1-3}$$

$$\frac{d\psi}{dz} = -\frac{\rho^2(1-\varepsilon)(\pi^2/4)\lambda\sin\theta}{\rho^2(1-\varepsilon)-(\pi^2\lambda u/4+\varepsilon\psi)^2} \tag{4}$$

subject to the boundary conditions:

$$u(0) = 0, \qquad \psi(0) = 0, \qquad \theta(0) = \alpha, \qquad \theta(1) = 0 \tag{5}$$

where ε and α are physical constants, and ψ is the dimensionless change in curvature. The variables in Fig. 1 are related to the dimensionless variables in Eqs. (1–5) by the following definitions: $W = \lambda W_{cri}$, W_{cri} = Euler's Buckling Load, $v = uL$, $s = zL$, L = length of bar, α = end slope.

For a given pair of values of ε and α, the eigenvalues, λ, for a range of values of ρ are sought. Thus, the parameter is identified as ρ. Physically, ρ is a dimensionless material constant defined by $\phi_0 L$ where ϕ_0 is defined in the moment, M, equation cited earlier.

Differentiating Eqs. (1–5) with respect to ρ, the following equations are obtained:

$$dU/dz = (\cos\theta)C, \qquad dC/dz = P, \qquad dL/dz = 0 \tag{6-8}$$

$$dP/dz = f_0 - f_L L - f_C C - f_U U - f_P P \tag{9}$$

subject to the boundary conditions:

$$U(0) = 0, \qquad P(0) = 0, \qquad C(0) = 0, \qquad C(1) = 0 \tag{10}$$

where

$$U = du/d\rho, \qquad C = d\theta/d\rho, \qquad P = d\psi/d\rho, \qquad L = d\lambda/d\rho \tag{11}$$

and

$$\begin{aligned} f_0 &= 2\rho(1-\varepsilon)(\pi^2/4)\lambda\sin\theta G^2/F^2 \\ f_L &= \rho^2(1-\varepsilon)(\pi^2/4)\sin\theta(F+2\lambda\pi^2/4uG)F^2 \\ f_C &= \rho^2(1-\varepsilon)(\pi^2/4)\lambda\cos\theta/F \\ f_U &= 2\rho^2(1-\varepsilon)\pi^4/16\lambda^2\sin\theta G/F^2 \\ f_P &= 2\rho^2(1-\varepsilon)(\pi^2/4)\lambda\sin\theta G\varepsilon/F^2 \end{aligned} \tag{12}$$

and

$$F = \rho^2(1-\varepsilon) - (\pi^2\lambda u/4 + \varepsilon\psi)^2 \tag{13}$$

$$G = \pi^2\lambda u/4 + \varepsilon\psi \tag{14}$$

Equations (6–8) are now linear, which can therefore be reduced to two initial value problems by separating the dependent variables as follows:

$$U = U_1 + sU_2, \qquad C = C_1 + sC_2, \qquad P = P_1 + sP_2, \qquad L = L_1 + sL_2 \tag{15}$$

Now identify:

$$s = L(0) \tag{16}$$

then the two initial value problems are:

$$dU_1/dz = (\cos\theta)C_1, \qquad dC_1/dz = P_1, \qquad dL_1/dz = 0$$

$$dP_1/dz = f_0 - f_L L_1 - f_C C_1 - f_U U_1 - f_P P_1 \tag{17-20}$$

$$U_1(0) = P_1(0) = C_1(0) = L_1(0) = 0$$

and

$$dU_2/dz = (\cos\theta)C_2, \qquad dC_2/dz = P_2, \qquad dL_2/dz = 0$$

$$dP_2/dz = -f_L L_2 - f_C C_2 - f_U U_2 - f_P P_2 \tag{21-24}$$

$$U_2(0) = P_2(0) = C_2(0) = 0, \qquad L_2(0) = 1$$

The value of s can be evaluated by using the boundary condition at $z = 1$, which gives:

$$C(1) = C_1(1) + sC_2(1) = 0$$

from which:

$$s = -C_1(1)/C_2(1) \tag{25}$$

Method of Solution

The solution procedure, similar to those in detail in Refs. 3–7, can be illustrated by an example. Consider the solutions of Eqs. (1–4) for $\alpha = 40°$ and $\varepsilon = 0.25$, and a range of ρ from 0.1349 to 0.45. The solution of these equations at the first value of ρ, namely, 0.1349, is known as $\rho = 0.1349$, $\lambda = 0.3822$.

With the eigenvalue λ at $\rho = 0.1349$ known, the functions u, θ and ψ for the range of $z = 0$ to $z = 1$ can be calculated by Eqs. (1–4). Using these functions in Eqs. (17–24), these equations can now be integrated for $\rho = 0.1349 + \Delta\rho$ to get U_i, C_i, P_i and L_i for $z = 0$ to $z = 1$ ($i = 1, 2$). The constant s can now be evaluated by Eq. (25). With s and the solutions of Eqs. (17–24) both known: U, C, P, and L can then be calculated from Eq. (15).

As a final step, integration of Eq. (14) gives the solutions of Eqs. (1–4) for $\rho = 0.1349 + \Delta\rho$ as:

$$u(z)\big|_{\rho=0.1349+\Delta\rho} = u(z)\big|_{\rho=0.1349} + U(z)\big|_{\text{from Eq. (15)}} \cdot \Delta\rho \tag{26}$$

and similar expressions for:

$$\theta(z)\big|_{\rho=0.1349+\Delta\rho} \qquad \text{and} \qquad \psi(z)\big|_{\rho=0.1349+\Delta\rho}$$

It is to be noted that the eigenvalue λ remains constant between $z = 0$ and $z = 1$ and is given by Eq. (16).

This procedure can be repeated to calculate the solutions of Eqs. (1–4) for $\rho = 0.1349 + 2\Delta\rho, 0.1349 + 3\Delta\rho, \ldots$, etc.

Results

Using the above noniterative method, solutions of Eqs. (1–4) were calculated for a wide range of values of the parameters. For comparison purposes, solutions of Eqs. (1–4) computed by the method of transformation groups as given in Ref. 1 are compared with results obtained by the present method. Selected results are shown in Table 1. The high degree of accuracy depicted is typical of that obtained by using this simple and straightforward method.

Table 1 Comparative results

	$\varepsilon = 0.50$				$\varepsilon = 0.75$		
α	ρ	λ(Ref. 1)	λ(Present)	α	ρ	λ(Ref. 1)	λ(Present)
40°	0.5180	0.8051	0.8012	40°	0.5618	0.9467	0.9440
	0.2772	0.6914	0.6900		0.3145	0.8899	0.8892
	0.2260	0.6641	0.6634		0.2594	0.8751	0.8747
	0.1951	0.6471	0.6469		0.2256	0.8656	0.8655
	0.1789	0.6381	0.6380		0.2072	0.8603	0.8603
80°	0.5284	0.8377	0.8347	80°	0.4598	1.0570	1.0560
	0.3321	0.7722	0.7710		0.3393	1.0358	1.0353
	0.2606	0.7469	0.7464		0.2808	1.0251	1.0249
	0.2068	0.7274	0.7271		0.2448	1.0184	1.0183
	0.1901	0.7212	0.7211		0.2247	1.0146	1.0146

References

[1] Kurajian, G. M. and Na, T. Y., "An Initial Value Method for the Solution of an Eigenvalue Problem in Solid Mechanics," *Transactions of the ASME*: Ser. E, *Journal of Applied Mechanics*, Vol. 39, No. 3, Sept. 1972, pp. 854–855.

[2] Oden, J. T. and Childs, S. B., "Finite Deflections of a Nonlinearly Elastic Bar," *Transactions of the ASME*: Ser. E: *Journal of Applied Mechanics*, Vol. 37, No. 1, March 1970, pp. 48–52.

[3] Rubbert, P. E. and Landahl, M. T., "Solution of Nonlinear Flow Problems Through Parametric Differentiation," *Physics of Fluids*, Vol. 10, No. 4, April 1967, pp. 831–835.

[4] Tan, C. W. and DiBiano, "A Parametric Study of Falkner-Skan Problem with Mass Transfer," *AIAA Journal*, Vol. 10, No. 7, July 1972, pp. 923–925.

[5] Narayana, C. L. and Ramamoorthy, P., "Compressible Boundary-Layer Equations Solved by the Method of Parameter Differentiation," *AIAA Journal*, Vol. 10, No. 8, Aug. 1972, pp. 1085–1086.

[6] Na, T. Y., "Comment on 'Compressible Boundary–Layer Equations Solved by the Method of Parameter Differentiation'," *AIAA Journal*, Vol. 11, No. 12, Dec. 1973, pp. 1790–1791.

[7] Na, T. Y. and Habib, I. S., "Non-Iterative Solution of Natural Convection Equations by Parameter Differentiation," *International Journal of Heat and Mass Transfer*, Vol. 17, No. 3, March 1974, pp. 253–254.

Entropy Layer on a Supersonic Plane Flat Nose at Incidence

R. D. ARCHER* AND D. S. BETTERIDGE†

University of New South Wales, Kensington, Australia

Nomenclature

d = model depth and reference length
n = probe station
p_o, T_o = freestream stagnation pressure, temperature
w = probe depth
α = model incidence
γ = ratio of specific heats
θ = probe angle
λ = total pressure ratio, probe to freestream

Subscript
m = value of θ, λ for max pitot pressure recovery

Received March 26, 1974; revision received July 22, 1974. This work is supported by Australian Research Grants Committee.

Index category: Supersonic and Hypersonic Flow.

* Associate Professor. Member AIAA.

† Professional Officer, School of Mechanical and Industrial Engineering.

Introduction

THE calculations of Swigart[1] and Webb et al.,[2] using an inverse method, predicted the existence of an entropy layer for blunt round axisymmetric bodies at incidence, wherein the maximum entropy does not wet the body surface. The thickness of the presumed layer would however be very small and difficult to detect for such bodies. The method of integral relations has also been used for blunt body calculations by Prosnak[3] on the one hand, who ignored the layer, and by others[4–6] who did not ignore the entropy layer but assumed a certain stagnation streamline shape. The time dependent computational method recently developed by Moretti[7–9] and Godunov's finite difference method[10] do not contain such a restraint, but their use has been confined to round nosed symmetric shapes. Furthermore, there does not appear to have been published any experimental evidence for such an entropy layer on either plane or axisymmetric blunt bodies. The plane flat plate with sharp corners, when placed in an extreme asymmetric attitude should lend itself well to a study of this question, provided that the entropy layer extends well into the inviscid region (Fig. 1).

Design of Experiment

On the assumption that both the entropy layer and boundary layer are thin compared with the shock layer thickness of about $\frac{1}{4}$ in. (6 mm) on the flat faced block [$d = \frac{3}{4}$ in. (19 mm)] for the conditions of the test, it was presumed that the streamlines of interest would be substantially parallel to the face as they passed the corner. The tests were performed in a $4 \times 5\frac{1}{2}$ in. (102×140 mm) test section at a Mach number $M = 3.08$ and a unit Reynolds number of 10^6/in. (4×10^7 per m). The freestream stagnation pressure and temperature were $p_0 = 75$ psia (517 *kPa*) and $T_0 = 520$ R (288 K).

Provided that the boundary–layer thickness remains small compared to that of the entropy layer, a total head probe traverse at the corner might be expected to reveal the true total pressure and hence entropy variation. The laminar boundary layer at the corner is estimated to be about 0.001 in. (0.025 mm) thick, for the conditions of this experiment. Thus, a carefully designed traverse mechanism having a read out accuracy of this order or better could detect the presence of an entropy layer thicker than about 0.0025 in. (0.06 mm). The accuracy claimed for this experiment is in fact of the order of 1/10 of this value.

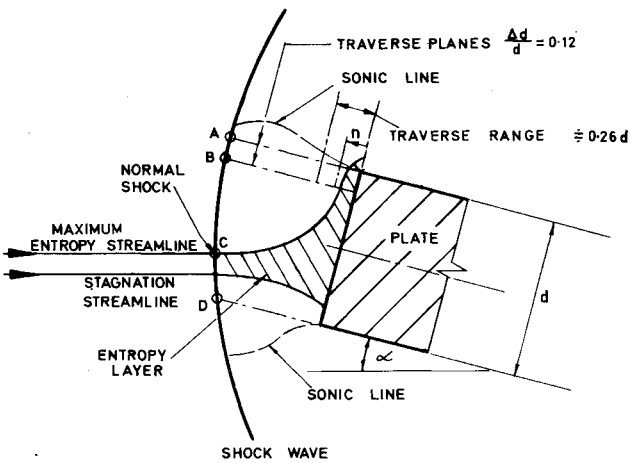

Fig. 1 Flat nosed plate at incidence in supersonic flow.